

## 以9,10-双(咪唑基)蒽为配体的锌配合物的合成、晶体结构和荧光性质

施梅 喻敏 刘光祥\*

(南京晓庄学院环境科学学院, 新型功能材料南京市重点实验室, 南京 211171)

**摘要:** 以9,10-双(咪唑基)蒽(DIA)和硝酸锌为原料, 分别与对苯二甲酸(H<sub>2</sub>bdc)、二苯甲酮-4,4'-二羧酸(H<sub>2</sub>cdc)、反式-1,4-环己二甲酸(H<sub>2</sub>chdc)在溶剂热条件下反应, 得到3个结构不同的配位聚合物[Zn<sub>2</sub>(DIA)(bdc)<sub>2</sub>]<sub>n</sub> (**1**)、{[Zn(DIA)(cdc)]·H<sub>2</sub>O}<sub>n</sub> (**2**)和[Zn(DIA)(chdc)]<sub>n</sub> (**3**)。对它们进行了X射线单晶衍射分析、元素分析、红外光谱分析和热重分析。单晶结构分析显示, 配合物**1**是第一例拥有三维(4,7)-连接的{3<sup>2</sup>.4.5<sup>2</sup>.6}{3<sup>2</sup>.4<sup>8</sup>.5<sup>4</sup>.6<sup>5</sup>.7<sup>2</sup>}<sub>2</sub>拓扑结构; 配合物**2**具有二维格子状结构, 层与层之间通过O-H...O和π...π弱相互作用形成三维超分子结构; 而配合物**3**具有二维两重贯穿的层状结构。结果说明有机羧酸的长度和刚性在配合物组装过程中起着非常重要的作用。此外, 在室温下对3个配合物进行了荧光性质分析。

**关键词:** 锌配合物; 双咪唑配体; 羧酸配体; 晶体结构; 荧光性质

中图分类号: O614.24<sup>+</sup>1

文献标识码: A

文章编号: 1001-4861(2020)12-2367-10

DOI: 10.11862/CJIC.2020.257

## Syntheses, Crystal Structures and Photoluminescent Properties of Three Zinc(II) Coordination Polymers Constructed from 9,10-Di(1*H*-imidazol-1-yl)anthracene

SHI Mei YU Min LIU Guang-Xiang\*

(Nanjing Key Laboratory of Advanced Functional Materials, School of Environmental Science,  
Nanjing Xiaozhuang University, Nanjing 211171, China)

**Abstract:** Three zinc(II) coordination polymers, [Zn<sub>2</sub>(DIA)(bdc)<sub>2</sub>]<sub>n</sub> (**1**), {[Zn(DIA)(cdc)]·H<sub>2</sub>O}<sub>n</sub> (**2**) and [Zn(DIA)(chdc)]<sub>n</sub> (**3**) (DIA=9,10-di(1*H*-imidazol-1-yl)anthracene, H<sub>2</sub>bdc=1,4-benzenedicarboxylic acid, H<sub>2</sub>cdc=4,4'-carbonyldibenzoic acid, H<sub>2</sub>chdc=*trans*-1,4-cyclohexanedicarboxylic acid), have been synthesized and characterized by IR spectroscopy, elemental analyses, thermogravimetric analyses and single-crystal X-ray diffraction. Structural analyses reveal that complex **1** displays an unprecedented three-dimensional (3D) (4,7)-connected framework featuring {3<sup>2</sup>.4.5<sup>2</sup>.6}{3<sup>2</sup>.4<sup>8</sup>.5<sup>4</sup>.6<sup>5</sup>.7<sup>2</sup>}<sub>2</sub> topology. Complex **2** has a two-dimensional (2D) structure, which is further packed into a 3D supramolecular architecture by intermolecular weak interactions, whereas complex **3** features a 2D two-fold interpenetrating layer structure. The results show that the length and the flexibility of the carboxylates exert obvious influence on the resulting architectures. Meanwhile, the photoluminescent properties of three complexes at room temperature were also investigated. CCDC: 1814085, **1**; 1814086, **2**; 1986966, **3**.

**Keywords:** zinc(II) coordination polymer; bis(imidazole) ligand; dicarboxylate; crystal structure; photoluminescence

Coordination polymers (CPs) are an emerging field of crystalline solid materials with well-organized network structures built by the linkage of metal ions/

clusters/chains/layers with organic ligands and have attracted great interest over the last few decades because of their multitudinous fascinating structures,

收稿日期: 2020-06-03。收修改稿日期: 2020-09-06。

国家自然科学基金(No.21671107)资助项目。

\*通信联系人。E-mail: njuliugx@126.com

unlimited tunability, and a wide variety of applications such as gas storage and separation, chemical sensing, heterogeneous catalysis, luminescence and magnetism<sup>[1-7]</sup>. Despite that a comparatively large number of interesting coordination polymers with intricate structural architectures have been reported to date, the design and construction of multi-functional CPs with desired structures and properties remains a significant challenge for chemists. This is because many intrinsic and external factors, such as the coordination nature of the metal ions, the structural characteristics of the organic ligands, stoichiometry, temperature, solvent and the pH of the solution, may considerably influence the formation of resulting CPs<sup>[8-16]</sup>. Of all the influencing factors, the deliberate selection of functionalized organic ligands plays a crucially important role in the structural assembly process, and in some cases, a subtle alteration of organic motifs may lead to a novel architecture<sup>[17-19]</sup>.

Recently, some coordination polymers based on  $\pi$ -conjugated molecules have been constructed and show superior physical properties<sup>[20-22]</sup>. As a crucial class of  $\pi$ -conjugated molecules, the anthracene derivatives possess unique properties in building luminescent materials. It should be an excellent strategy to synthesize luminescent materials with outstanding sensing properties through the incorporation of anthracene moieties into networks<sup>[23-28]</sup>. Meanwhile, the five-membered heterocycles, such as imidazole, triazole and tetrazoles, are promising candidates in the design and fabrication of luminescent CPs<sup>[29-32]</sup>. Keeping the aforementioned reasons in mind, we select the ligand 9,10-bis(1*H*-imidazol-1-yl)-anthracene (DIA), in which the anthracene spacers are directly bonded to the imidazole as bulky bis(imidazole) ligand to obtain microporous luminescent materials<sup>[33-36]</sup>. In this work, three coordination polymers,  $[\text{Zn}_2(\text{DIA})(\text{bdc})_2]_n$  (**1**),  $\{[\text{Zn}(\text{DIA})(\text{cdc})] \cdot \text{H}_2\text{O}\}_n$  (**2**) and  $[\text{Zn}(\text{DIA})(\text{chdc})]_n$  (**3**), have been synthesized by using DIA ligand and different dicarboxylic acid, where  $\text{H}_2\text{bdc}$ =1,4-benzenedicarboxylic acid,  $\text{H}_2\text{cdc}$ =4,4'-carbonyldibenzoic acid and  $\text{H}_2\text{chdc}$ =*trans*-1,4-cyclohexanedicarboxylic acid. The effects of anions on their structures are unraveled in detail. Moreover, the photo-

luminescent properties of three complexes have also been studied.

## 1 Experimental

### 1.1 Materials and general methods

All chemicals and solvents were of reagent grade and used as received without further purification. The DIA ligand was synthesized according to the reported method<sup>[34]</sup>. Elemental analyses (C, H and N) were performed on a Vario EL III elemental analyzer. Infrared spectra were recorded on KBr discs using a PerkinElmer Frontier FT-IR spectrometer in a range of 4 000~400  $\text{cm}^{-1}$ . Thermogravimetric analyses (TGA) were performed on a Netzsch STA-409PC instrument in flowing  $\text{N}_2$  with a heating rate of 10  $^\circ\text{C} \cdot \text{min}^{-1}$ . The luminescent spectra for the powdered samples were measured at ambient temperature on a Horiba FluoroMax-4P-TCSPC fluorescence spectrophotometer. All the measurements were carried out under the same experimental conditions.

### 1.2 Synthesis of $[\text{Zn}_2(\text{DIA})(\text{bdc})_2]_n$ (**1**)

A mixture containing  $\text{Zn}(\text{NO}_3)_2 \cdot 6\text{H}_2\text{O}$  (29.7 mg, 0.1 mmol),  $\text{H}_2\text{bdc}$  (16.6 mg, 0.1 mmol), and DIA (31.0 mg, 0.1 mmol) in DMF/ $\text{H}_2\text{O}$  (1:1, *V/V*) solution (10 mL) was sealed in a Teflon-lined stainless steel container and heated at 150  $^\circ\text{C}$  for 3 d. After being cooled down to room temperature, light yellow pillar crystals of **1** were obtained in 41% yield based on DIA. Anal. Calcd. for  $\text{C}_{36}\text{H}_{22}\text{N}_4\text{O}_8\text{Zn}_2$ (%): C, 56.20; H, 2.88; N, 7.2. Found(%): C, 56.15; H, 2.91; N, 7.26. IR (KBr,  $\text{cm}^{-1}$ ): 3 432 (m), 3 046 (w), 1 621 (s), 1 559 (s), 1 523 (s), 1 444 (s), 1 422 (m), 1 403 (m), 1 392 (s), 1306 (m), 1 217 (m), 1 091 (m), 1 021 (w), 937 (w), 822 (m), 743 (m), 665 (w), 541 (w).

### 1.3 Synthesis of $\{[\text{Zn}(\text{DIA})(\text{cdc})] \cdot \text{H}_2\text{O}\}_n$ (**2**)

Complex **2** was prepared by using a method similar to that used for the preparation of **1**, except that  $\text{H}_2\text{cdc}$  (27.0 mg, 0.1 mmol) was used instead of  $\text{H}_2\text{bdc}$ . Colorless block crystals of **2** were collected by filtration and washed with water and ethanol several times with a yield of 62% based on DIA ligand. Anal. Calcd. for  $\text{C}_{35}\text{H}_{24}\text{N}_4\text{O}_6\text{Zn}$ (%): C, 65.50; H, 3.65; N, 8.46. Found (%): C, 65.52; H, 3.66; N, 8.47. IR (KBr,  $\text{cm}^{-1}$ ): 3 427

(m), 3 065 (m), 1 687 (s), 1 583 (m), 1 521 (s), 1 453 (m), 1 387 (s), 1 251 (m), 1 081 (m), 948 (m), 831 (w), 763 (s), 662 (m), 523 (w).

#### 1.4 Synthesis of [Zn(DIA)(chdc)]<sub>n</sub> (**3**)

The procedure for the synthesis of **3** was similar to that used for **1**, except that H<sub>2</sub>chdc (17.2 mg, 0.1 mmol) was used instead of H<sub>2</sub>bdc. Light yellow block crystals of **3** were collected by filtration and washed with water and ethanol several times with a yield of 51% based on DIA ligand. Anal. Calcd. for C<sub>28</sub>H<sub>24</sub>N<sub>4</sub>O<sub>4</sub>Zn(%): C, 61.60; H, 4.43; N, 10.26. Found(%): C, 61.55; H, 4.45; N, 10.28. IR (KBr, cm<sup>-1</sup>): 3 471 (m), 3 053 (m), 2 927 (w), 1 587 (m), 1 518 (s), 1 445 (m), 1 379 (s), 1 263 (m), 1 091 (s), 1 022 (m), 954 (m), 862 (w), 737 (s), 631 (m), 539 (w).

#### 1.5 X-ray crystallography

Single-crystal X-ray diffraction data for **1**~**3** was collected on a Bruker SMART APEX II CCD diffrac-

tometer equipped with a graphite-monochromatic Mo K $\alpha$  radiation ( $\lambda=0.071\ 073$  nm) using the  $\varphi$ - $\omega$  scan mode at 293(2) K. The diffraction data were integrated by using the SAINT program<sup>[37]</sup>, which was also used for the intensity corrections for the Lorentz and polarization effects. Semi-empirical absorption corrections were applied using the SADABS program<sup>[38]</sup>. The structures were solved by direct methods using SHELXS-2014<sup>[39]</sup> and all the non-hydrogen atoms were refined anisotropically on  $F^2$  by the full-matrix least-squares technique with the SHELXL-2014<sup>[40]</sup> crystallographic software package. The hydrogen atoms, except those of water molecules, were generated geometrically and refined isotropically using the riding model. The pertinent crystallographic data collection and structure refinement parameters are presented in Table 1 and selected bond lengths and angles are listed in Table 2.

CCDC: 1814085, **1**; 1814086, **2**; 1986966, **3**.

Table 1 Crystal data and structure refinements for complexes **1**~**3**

Complex	<b>1</b>	<b>2</b>	<b>3</b>
Formula	C <sub>36</sub> H <sub>22</sub> N <sub>4</sub> O <sub>8</sub> Zn <sub>2</sub>	C <sub>35</sub> H <sub>24</sub> N <sub>4</sub> O <sub>6</sub> Zn	C <sub>28</sub> H <sub>24</sub> N <sub>4</sub> O <sub>4</sub> Zn
Formula weight	769.31	661.95	545.88
Crystal system	Monoclinic	Triclinic	Monoclinic
Space group	$P2_1/c$	$P\bar{1}$	$C2/c$
$a$ / nm	0.978 53(17)	1.059 55(17)	1.278 22(13)
$b$ / nm	2.164 1(4)	1.268 8(2)	2.521 8(3)
$c$ / nm	1.476 7(3)	1.307 3(2)	0.814 84(9)
$\alpha$ / (°)		110.794(4)	
$\beta$ / (°)	103.332(5)	102.388(4)	106.977(2)
$\gamma$ / (°)		105.517(4)	
$V$ / nm <sup>3</sup>	3.042 8(9)	1.486 8(4)	2.512 1(5)
$Z$	4	2	4
$D_c$ / (g·cm <sup>-3</sup> )	1.679	1.479	1.443
Absorption coefficient / mm <sup>-1</sup>	1.641	0.881	1.020
$\theta$ range / (°)	2.85~25.50	2.90~27.66	2.94~25.03
$F(000)$	1 560	680	1 128
Reflection collected	37 002	21 278	13 085
Independent reflection	5 655 ( $R_{int}=0.028\ 5$ )	6 868 ( $R_{int}=0.060\ 4$ )	2 220 ( $R_{int}=0.116\ 2$ )
Reflection observed [ $I>2\sigma(I)$ ]	4 878	5 060	1 910
Data, restraint, parameter	5 655, 0, 451	6 868, 0, 415	2 220, 0, 169
Goodness-of-fit on $F^2$	1.064	1.070	1.188
$R_1, wR_2$ [ $I>2\sigma(I)$ ]	0.028 9, 0.065 6	0.056 0, 0.110 3	0.094 1, 0.134 5
$R_1, wR_2$ (all data)	0.037 8, 0.069 3	0.086 5, 0.119 7	0.121 7, 0.144 2
Largest diff. peak and hole / (e·nm <sup>-3</sup> )	417, -390	529, -412	1 114, -808

Table 2 Selected bond lengths (nm) and angles (°) for complexes 1~3

1					
Zn(1)-O(1)	0.192 02(17)	Zn(1)-O(6)	0.197 69(16)	Zn(1)-N(1)	0.200 17(19)
Zn(1)-O(4)#1	0.201 13(16)	Zn(2)-O(7)	0.193 52(17)	Zn(2)-O(5)#3	0.209 98(16)
Zn(2)-O(3)	0.201 45(17)	Zn(2)-O(2)#4	0.244 7(2)	Zn(2)-N(4)#2	0.204 03(19)
O(1)-Zn(1)-O(6)	100.95(8)	O(1)-Zn(1)-O(4)#1	109.28(8)	O(1)-Zn(1)-N(1)	127.49(8)
O(6)-Zn(1)-O(4)#1	97.41(7)	O(6)-Zn(1)-N(1)	117.84(8)	N(1)-Zn(1)-O(4)#1	99.76(7)
O(7)-Zn(2)-O(3)	115.87(8)	N(4)#2-Zn(2)-O(5)#3	99.53(7)	O(7)-Zn(2)-N(4)#2	125.16(9)
O(7)-Zn(2)-O(2)#4	78.00(7)	O(3)-Zn(2)-N(4)#2	116.97(7)	O(3)-Zn(2)-O(2)#4	85.26(7)
O(7)-Zn(2)-O(5)#3	101.09(7)	N(4)#2-Zn(2)-O(2)#4	92.65(7)	O(3)-Zn(2)-O(5)#3	82.07(7)
O(5)#3-Zn(2)-O(2)#4	165.40(7)				
2					
Zn(1)-N(1)	0.202 2(2)	Zn(1)-O(1)	0.193 1(2)	Zn(1)-N(4)#1	0.203 0(2)
Zn(1)-O(3)#2	0.197 5(2)				
N(1)-Zn(1)-N(4)#1	106.41(10)	O(1)-Zn(1)-O(3)#2	105.16(10)	O(1)-Zn(1)-N(1)	125.28(11)
O(3)#2-Zn(1)-N(1)	105.20(10)	O(1)-Zn(1)-N(4)#1	100.40(10)	O(3)#2-Zn(1)-N(4)#1	114.92(10)
3					
Zn(1)-O(1)	0.195 9(3)	Zn(1)-O(1)#1	0.195 9(3)	Zn(1)-N(1)#1	0.199 9(4)
Zn(1)-N(1)	0.200 0(4)				
O(1)-Zn(1)-O(1)#1	98.3(2)	O(1)-Zn(1)-N(1)	109.48(17)	O(1)-Zn(1)-N(1)#1	107.74(17)
O(1)#1-Zn(1)-N(1)	107.74(17)	O(1)#1-Zn(1)-N(1)#1	109.48(17)	N(1)#1-Zn(1)-N(1)	121.6(3)

Symmetry codes: #1:  $x+1, y, z$ ; #2:  $-x+1, y-1/2, -z+3/2$ ; #3:  $x-1, -y+3/2, z-1/2$ ; #4:  $x-1, y, z$  for **1**; #1:  $x, y+1, z$ ; #2:  $x-1, y, z-1$  for **2**; #1:  $-x+1, y, -z+1/2$  for **3**.

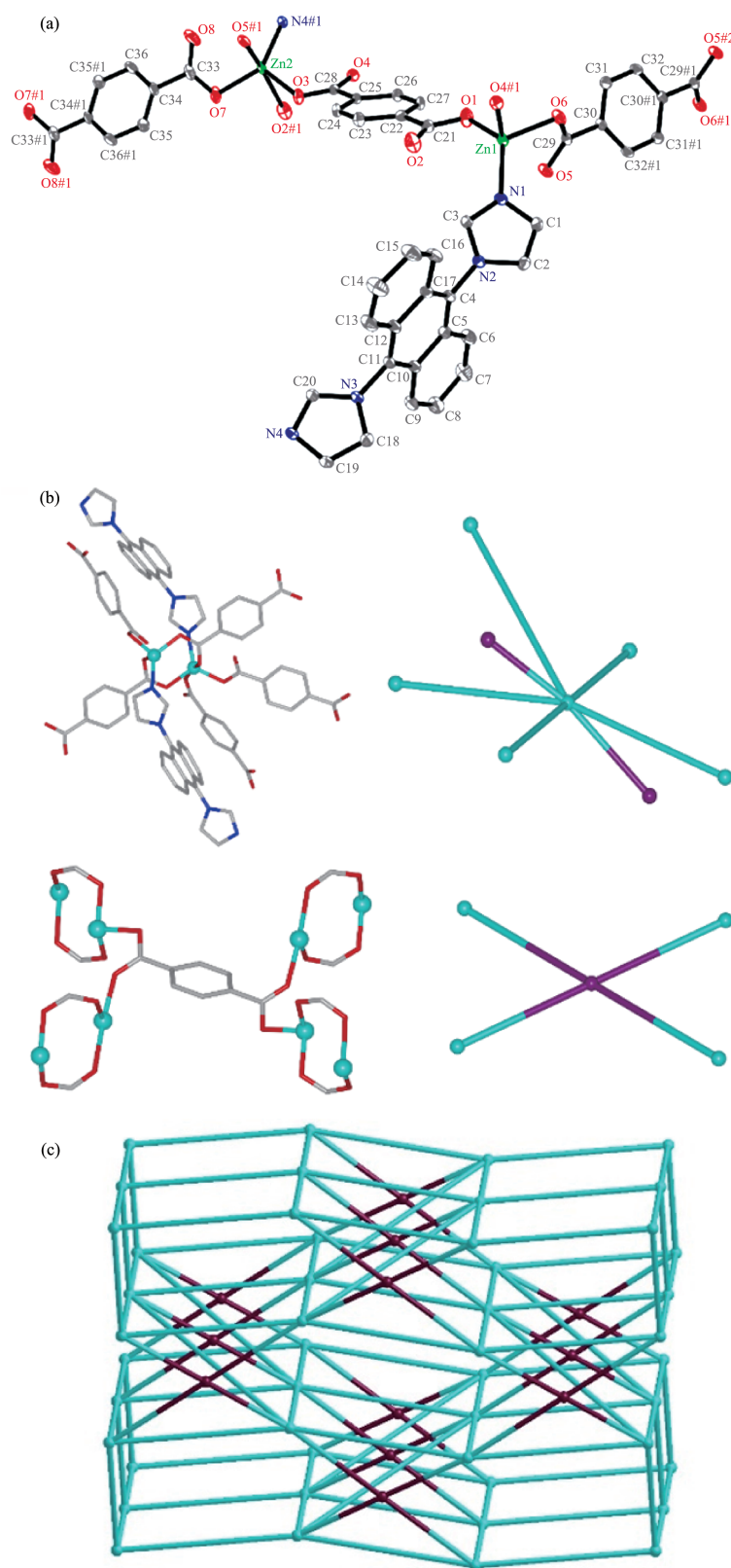
## 2 Results and discussion

### 2.1 Crystal structure

Single crystal X-ray diffraction analysis revealed that complex **1** crystallizes in the monoclinic space group  $P2_1/c$ . The asymmetric unit of complex **1** contains two crystallography independent Zn(II) ions, one unique DIA ligand, one  $\text{bdc}^{2-}$  anion and two half  $\text{bdc}^{2-}$  anions which are located at an inversion center as illustrated in Fig. 1a. The Zn1 ion is four-coordinated by one nitrogen atom from DIA ligand and three carboxylate oxygen atoms from three individual  $\text{bdc}^{2-}$  anions, conforming a distorted tetrahedrally geometry. The Zn2 ion is five-coordinated by one nitrogen atom from DIA ligand, and four oxygen atoms from four different  $\text{bdc}^{2-}$  anions in a distorted trigonal bipyramidal geometry with a  $\tau$  value of 0.632<sup>[41]</sup>. The Zn-O bond lengths are in a range of 0.192 02(17)~0.244 7(2) nm, the Zn-N bond lengths are between 0.200 17(19) and 0.204 03(19)

nm, and the coordination angles around Zn(II) ions span from 78.00(7)° to 165.40(7)°. The Zn-N and Zn-O bond lengths and the bond angles around Zn(II) ions in **1** are comparable with other Zn(II) coordination polymers<sup>[22]</sup>.

The DIA ligand exhibits a *cis*-conformation with interplanar angle between imidazole and anthracene of 71.05° and 77.94°, which is first example up to now. Each DIA ligand links two Zn(II) ions with a separation of 1.303 6(5) nm. For the three asymmetric  $\text{bdc}^{2-}$  anions, two of them adopt a bridging mode of  $\mu_4\text{-}\eta^1\text{:}\eta^1\text{:}\eta^1\text{:}\eta^1$  to link four Zn(II) ions, and the other uses a bridging mode of  $\mu_2\text{-}\eta^1\text{:}\eta^0\text{:}\eta^1\text{:}\eta^0$  to connect two Zn(II) ions. Two Zn(II) ions are linked by a pair of carboxylate groups to form a binuclear  $\text{Zn}_2$  unit, with a  $\text{Zn1}\cdots\text{Zn2}$  distance of 0.430 5(8) nm. Each binuclear unit is surrounded by seven organic ligands (two DIA ligands and five  $\text{bdc}^{2-}$  anions) to produce a three-dimensional (3D) framework. Topologically, the  $\mu_4\text{-}\eta^1\text{:}\eta^1\text{:}\eta^1\text{:}\eta^1\text{-bdc}$



Symmetry codes: #1:  $x+1, y, z$ ; #2:  $-x+1, y-1/2, -z+3/2$

Fig.1 (a) Coordination environments of Zn(II) ion in **1** with ellipsoids drawn at 30% probability level, where hydrogen atoms are omitted for clarity; (b) Perspective and schematic views of 4- and 7-connected nodes of **1**; (c) Schematic representation of (4,7)-connected framework with  $\{3^2.4.5^2.6\}\{3^2.4^8.5^4.6^5.7^2\}_2$  topology of **1**

anion can be considered as a 4-connected node, the  $\mu_2$ - $\eta^1:\eta^0:\eta^1:\eta^0$ -bdc anion and DIA ligand can be considered as linkers, and  $\text{Zn}_2$  units can be regarded as 7-connected nodes (Fig. 1b). Therefore, the 3D framework of **1** is (4,7)-connected topology with Schläfli symbol of  $\{3^2.4.5^2.6\}\{3^2.4^8.5^4.6^5.7^2\}_2$  which is, as expected, unique so far (Fig. 1c).

In order to investigate the influence of dicarboxylate ligand on the resulting framework of CPs, another dicarboxylate ligand,  $\text{H}_2\text{cdc}$ , which is longer and more flexible than  $\text{H}_2\text{bdc}$ , was utilized. Then we obtained complex **2** and it crystallizes in the triclinic space group  $P\bar{1}$  with one  $\text{Zn}(\text{II})$  ion, one  $\text{cdc}^{2-}$  anion, and one lattice water molecule in the asymmetric unit.  $\text{Zn}(\text{II})$  ion sits in the center of a distorted tetrahedron constructed

from two nitrogen atoms belonging to two symmetry related DIA ligands and two oxygen atoms of two individual  $\text{cdc}^{2-}$  anions.

The coordination modes of the two carboxylates from  $\text{cdc}^{2-}$  anion adopts monodentate mode. Both  $\text{cdc}^{2-}$  and DIA ligands are simultaneously coordinated to two  $\text{Zn}(\text{II})$  ions, which, for their part, are surrounded by four ligands in total. The  $\text{Zn}-\text{O}$  distances lie in a range of 0.193 1(2)~0.197 5(2) nm, whereas the  $\text{Zn}-\text{N}$  distances are 0.202 2(2) and 0.203 0(2) nm, respectively. The separation of  $\text{Zn}(\text{II})$  ions along the bridge formed by DIA and  $\text{cdc}$  ligands are of 1.268 80(21) and 1.495 78(19) nm, respectively. The DIA ligand adopts a *cis*-conformation with torsion angles of imidazole with respect to anthracene planes 63.66° and 83.01°, which

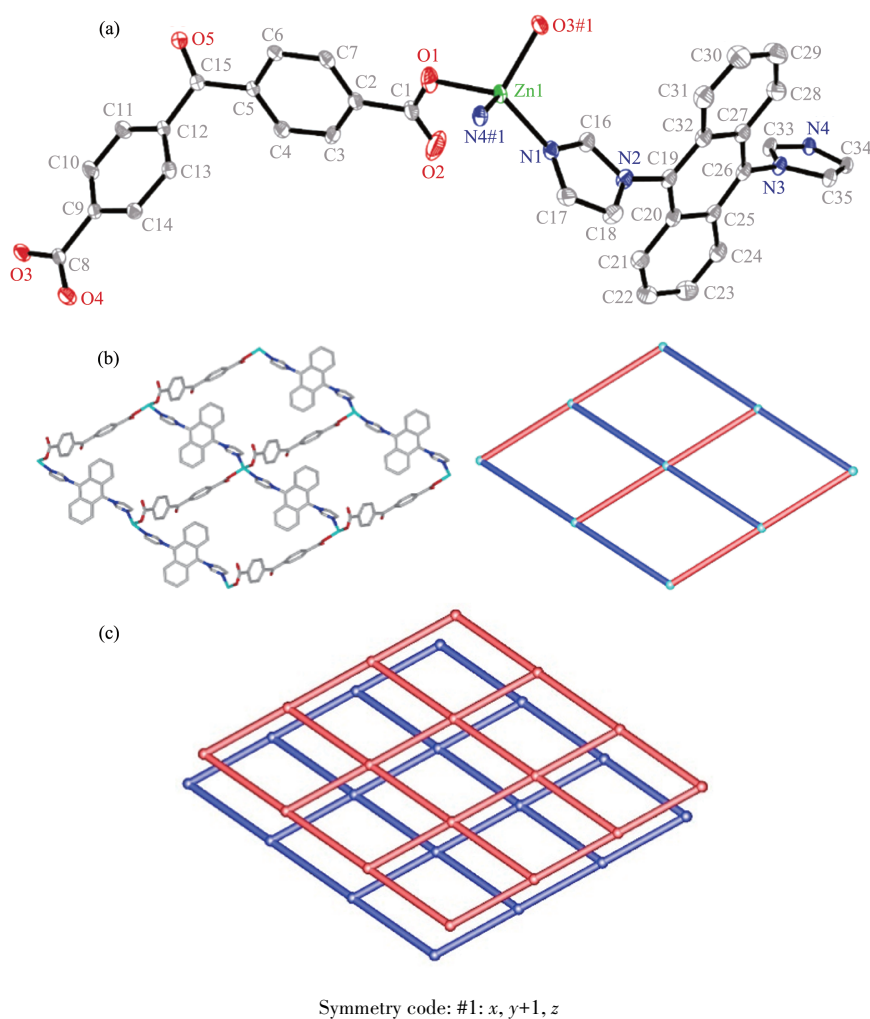


Fig. 2 (a) Coordination environments of the  $\text{Zn}(\text{II})$  ion in **2** with ellipsoids drawn at 30% probability level, where hydrogen atoms and lattice water molecules are omitted for clarity; (b) Perspective view of 2D layer structure of **2**; (c) Schematic representation of 2D (4,4) framework in **2**

is similar to that of **1**. The flexibility of  $\text{cdc}^{2-}$  anions is reflected in the Zn-C-Zn angle of  $127.59^\circ$ . Two-dimensional network is shown in Fig.2b, where the presence of chains formed by alternating Zn-DIA-Zn and Zn- $\text{cdc}^{2-}$ -Zn units is highlighted (DIA and  $\text{cdc}^{2-}$  ligands are represented in red and blue, respectively). In  $bc$  plane, these chains form 2D sheets that resemble a herringbone structure, with the ligands acting as linkers, and Zn(II) ions as nodes. Thereby, the overall structure can be described as a 4-connected, unimodal net of topological type  $4^4\text{-sql}$  (Fig.2b).

In the crystal, adjacent 2D layers are stacked in an ABAB... staggering mode and further packed into a 3D supramolecular architecture by O-H...O, C-H... $\pi$ ,  $\pi$ ... $\pi$  stacking noncovalent interactions (Fig. 2c). There exist strong O-H...O hydrogen-bonding interactions among the oxygen atoms of lattice water molecules and the carboxylate oxygen atoms. The C-H... $\pi$  interactions of 0.373 9 nm are observed between the C-H bond belonging to the benzene ring of  $\text{cdc}^{2-}$  anion and the anthracene ring of DIA ligand. Whereas,  $\pi$ ... $\pi$  interactions are seen between the neighboring benzene rings of DIA ligand with ring centroids separated by a

distance of 0.401 8 nm.

The use of flexible  $\text{H}_2\text{chdc}$  ligand results in a 2D two-fold interpenetrated topology of complex **3**. The structure analysis reveals that complex **3** crystallizes in the monoclinic space group  $C2/c$ , the asymmetric unit consists of one crystallographically independent Zn(II) ion lying on the 2-fold axis, one individual 1,4- $\text{chdc}^{2-}$  anions locating at an inversion center, and one DIA ligand situated at the 2-fold axis. As illustrated in Fig. 3a, the Zn(II) ion displays a distorted tetrahedral geometry, being surrounded by two carboxylic oxygen atoms from two different  $\text{chdc}^{2-}$  anions and two nitrogen atoms from two distinct DIA ligands. The Zn-O bond lengths are 0.195 9(3) nm, the Zn-N bond lengths are between 0.199 9(4) and 0.200 0(4) nm, and the coordination angles around Zn(II) ions span from  $98.3(2)^\circ$  to  $121.6(3)^\circ$ .

The DIA ligand exhibits a *trans*-conformation with interplanar angle between imidazole and anthracene of  $82.02^\circ$ , which is different from those of **1** and **2**. The  $\text{chdc}^{2-}$  anion adopts comparatively stable chair conformation and connects two Zn(II) ions through two monodentate carboxylates. Each Zn(II) ion is connected to

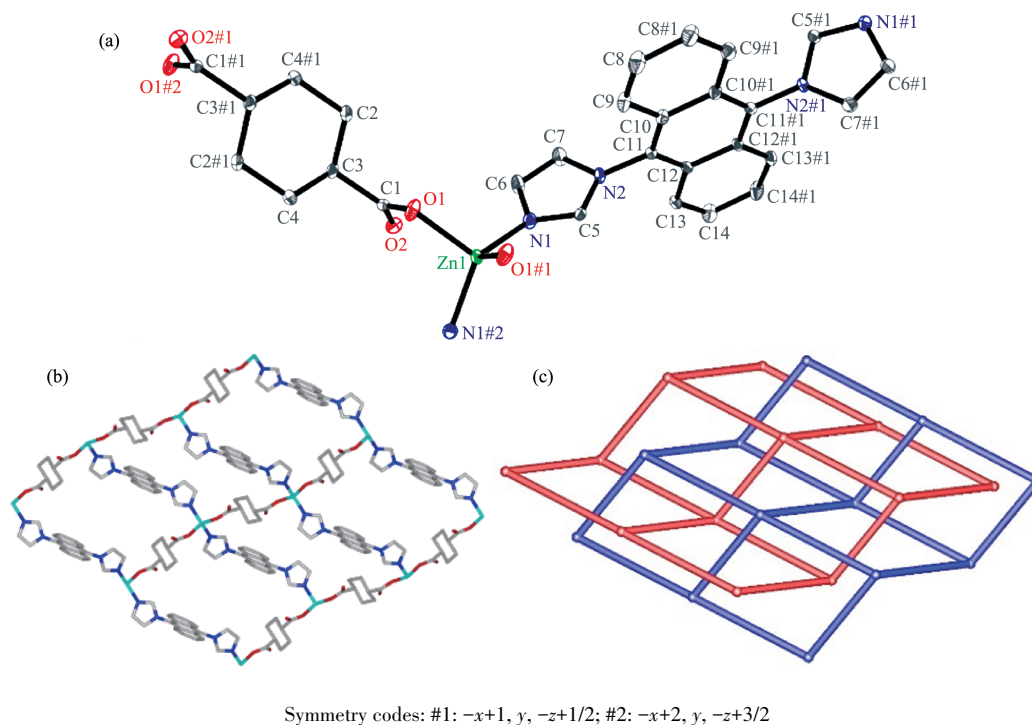


Fig.3 (a) Coordination environments of Zn(II) ion in **3** with ellipsoids drawn at 30% probability level, where hydrogen atoms are omitted for clarity; (b) View of 2D  $[\text{Zn}(\text{DIA})(\text{chdc})]_n$  network of **3**; (c) 2D+2D  $\rightarrow$  2D interpenetration network in **3**

two different  $\text{chdc}^{2-}$  anions and each  $\text{chdc}^{2-}$  anion is connected to two Zn(II) ions, building up a 1D chain, which are further connected by DIA ligands to form a 2D puckered sheet (Fig.3b). There is a large window in the puckered sheet with dimensions of  $1.369 \text{ nm} \times 1.953 \text{ nm}$ . Within the sheet, the Zn(II) ions are not all coplanar, rather, half fall in one plane, half in the other parallel plane. The puckered nature of the sheets with large square windows may offer a good chance to generate a  $2\text{D}+2\text{D} \rightarrow 2\text{D}$  interpenetration bilayer structure with a  $\{4^4.6^2\}$  topology (Fig.3c).

More interestingly, the neighboring 2D sheets are staggered parallel with each other. The 2D layers are sustained by  $\pi \cdots \pi$  interactions between the neighboring benzene rings of DIA ligand with ring centroids separated by a distance of  $0.416 \text{ nm}$  and  $\text{C-H} \cdots \pi$  interactions among the DIA ligands. Obviously, this packing mode decreases the molecular repulsion and stabilizes the whole structure of **3**.

## 2.2 FTIR spectra

The IR spectra of **1**~**3** showed the absence of the characteristic bands at around  $1700 \text{ cm}^{-1}$  attributed to the protonated carboxylate group, which indicates the complete deprotonation of  $\text{H}_2\text{bdc}$ ,  $\text{H}_2\text{cdc}$  and  $\text{H}_2\text{chdc}$  ligands upon reaction with Zn(II) ion. The presence of vibrational bands  $1650\sim 1550 \text{ cm}^{-1}$ , which are characteristic of the asymmetric stretching of the deprotonated carboxylic groups of  $\text{bdc}^{2-}$ ,  $\text{cdc}^{2-}$  and  $\text{chdc}^{2-}$  anions. The difference between asymmetric and symmetric carbonyl stretching frequencies ( $\Delta\nu = \nu_{\text{asym}} - \nu_{\text{sym}}$ ) was used to fetch information on the metal-carboxylate binding modes. Complex **1** showed two pairs of  $\nu_{\text{asym}}$  and  $\nu_{\text{sym}}$  frequencies at  $1621, 1422 \text{ cm}^{-1}$  ( $\Delta\nu = 199 \text{ cm}^{-1}$ ) and  $1559, 1392 \text{ cm}^{-1}$  ( $\Delta\nu = 167 \text{ cm}^{-1}$ ) for the carbonyl functionality indicating two coordination modes as observed in the crystal structure. Complex **2** showed a pair of  $\nu_{\text{asym}}$  and  $\nu_{\text{sym}}$  frequencies at  $1583, 1387 \text{ cm}^{-1}$  ( $\Delta\nu = 196 \text{ cm}^{-1}$ ) corresponding to the carbonyl functionality of dicarboxylate ligand indicating a symmetric monodentate coordination mode. Complex **3** showed a pair of  $\nu_{\text{asym}}$  and  $\nu_{\text{sym}}$  frequencies at  $1587, 1379 \text{ cm}^{-1}$  ( $\Delta\nu = 208 \text{ cm}^{-1}$ ) corresponding to the carbonyl functionality of dicarboxylate ligand indicating a symmetric monodentate

coordination mode. The OH stretching broad bands at  $3427 \text{ cm}^{-1}$  for **2** are attributable to the lattice water. The bands in the region of  $630\sim 1270 \text{ cm}^{-1}$  are attributed to the -CH- in-plane or out-of-plane bend, ring breathing, and ring deformation absorptions of benzene ring, respectively. The IR spectra exhibit the characteristic peaks of imidazole groups at *ca.*  $1520 \text{ cm}^{-1}$  [42].

## 2.3 Thermal stability

To examine the thermal stabilities of three complexes, thermogravimetric analyses (TGA) were carried out at a heating rate of  $10 \text{ }^\circ\text{C} \cdot \text{min}^{-1}$  under a dry air atmosphere at the temperature from  $20$  to  $800 \text{ }^\circ\text{C}$ . As shown in Fig.4, the TGA curve of **1** revealed that no obvious weight loss was observed until the temperature rose to  $280 \text{ }^\circ\text{C}$ . The anhydrous compound decomposed from  $280$  to  $800 \text{ }^\circ\text{C}$ , indicating the release of organic components. For **2**, the first weight loss of  $2.44\%$  (Calcd.  $2.39\%$ ) occurred in a range of  $55$  to  $150 \text{ }^\circ\text{C}$ , indicating the loss of one free water molecules. Then, the framework of **2** decomposed gradually above  $245 \text{ }^\circ\text{C}$ . Complex **3** was stable up to *ca.*  $240 \text{ }^\circ\text{C}$ , and the framework collapsed in a temperature range of  $240\sim 800 \text{ }^\circ\text{C}$  before the final formation of a metal oxide.

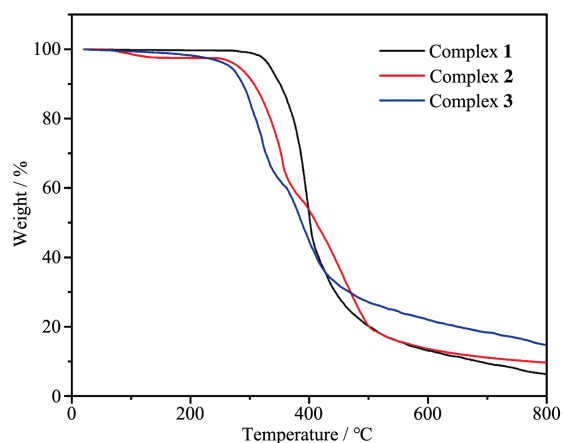


Fig.4 TGA curves of complexes **1**~**3**

## 2.4 Photoluminescent properties

Photoluminescent properties of Zn(II) complexes have attracted intense interest due to their potential applications in photochemistry, chemical sensors, and electroluminescent display [43-47]. The photoluminescent properties of **1**~**3** and DIA ligand were investigated in

solid state at room temperature. The DIA ligand exhibited emission band with a maximum at 474 nm upon excitation at 370 nm, which may be assigned to  $\pi^* \rightarrow n$  or  $\pi^* \rightarrow \pi$  transitions of the ligand<sup>[48-50]</sup>.

As shown in Fig. 5a, the emission peaks of three complexes occurred at 428 nm ( $\lambda_{\text{ex}}=365$  nm) for **1**, 442 nm ( $\lambda_{\text{ex}}=370$  nm) for **2** and 454 nm ( $\lambda_{\text{ex}}=377$  nm) for **3**. Under the same experimental conditions, the emission intensities from free H<sub>2</sub>bdc, H<sub>2</sub>cdc and H<sub>2</sub>chdc are much weaker than that from DIA ligand, so it is considered that they has no significant contribution to the fluorescent emission of the complexes in the presence of DIA ligand. Comparison to free DIA ligand, the emission peaks for **1~3** were blue-shifted by *ca.* 47, 33 and 21 nm, respectively. These emissions are neither metal-to-ligand charge transfer (MLCT) nor ligand-to-metal charge transfer (LMCT) in nature, since Zn(II) ion is difficult to oxidize or reduce due to its  $d^{10}$  configuration<sup>[51-53]</sup>. The photoluminescent of **1~3** may originate from the intraligand  $\pi^* \rightarrow \pi$  or  $\pi^* \rightarrow n$  transition since similar emissions were also observed for the ligands

themselves. The emission discrepancy of these complexes is probably due to the different configurations of DIA ligand, the differences of organic ligands and coordination environments of central metal ions, which have a close relationship to the photoluminescence behavior<sup>[54-55]</sup>. The chromaticity coordinates for **1~3** are (0.234 7, 0.234 6), (0.218 7, 0.201 6) and (0.230 5, 0.255 9), respectively (Fig. 5b). As we know that the luminescence characteristic of CPs is closely related to their structures<sup>[56]</sup>. The size of the metal, the structure of the secondary building units (SBUs) and the orientation of the linkers all affect the emission properties of the material<sup>[57-60]</sup>. Complexes **1~3** contain the same linker (DIA) in different configurations, allowing comparative study of their photoluminescence diversity. The different visual fluorescence may be attributed to the various structures of three complexes (**1**: 3D, **2**: 2D, **3**: 2D). The enhancement of their emission intensity compared with that of DIA ligand can be properly attributed to the increased rigidity of DIA ligand when binding to Zn(II) ion, which will effectively reduce the loss of energy.

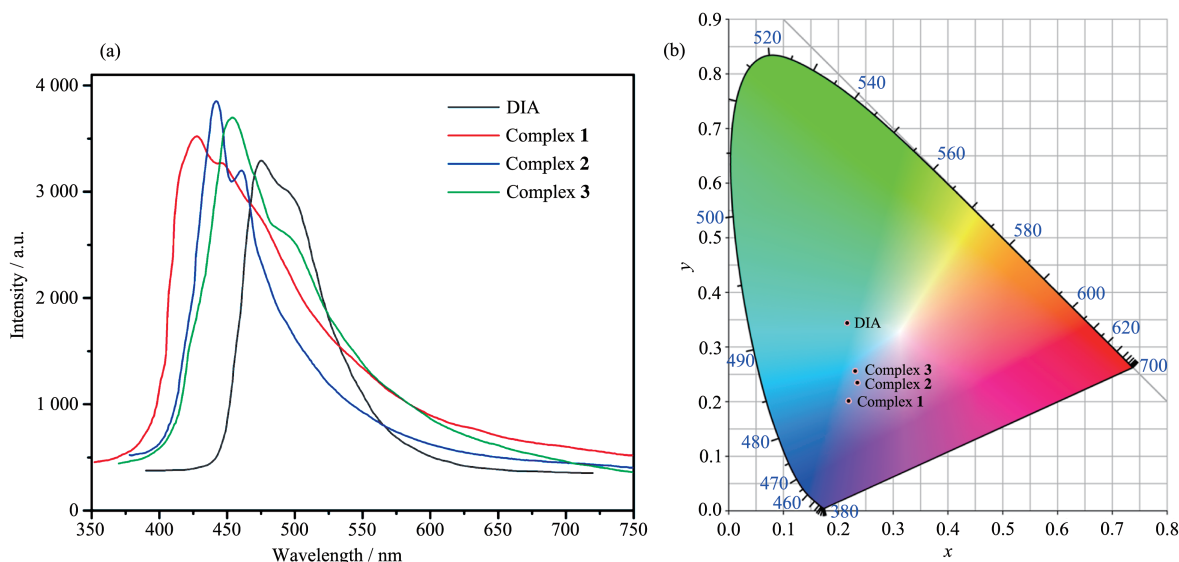


Fig.5 (a) Solid-state photoluminescent spectra of complexes **1~3** and DIA ligand; (b) CIE chromaticity diagrams of complexes **1~3** and DIA ligand

## References:

[1] Furukawa H, Cordova K E, O'Keeffe M, et al. *Science*, **2013**, **341**:1230444  
 [2] Noh T H, Jung O S. *Acc. Chem. Res.*, **2016**, **49**:1835-1843  
 [3] Zhou H C, Long J R, Yaghi O M. *Chem. Rev.*, **2012**, **112**:673-

674

[4] Li P, Vermeulen N A, Malliakas C D, et al. *Science*, **2017**, **356**:624-627  
 [5] Islamoglu T, Goswami S, Li Z, et al. *Acc. Chem. Res.*, **2017**, **50**:805-813  
 [6] Cui Y, Li B, He H, et al. *Acc. Chem. Res.*, **2016**, **49**:483-493

- [7] Hu Z, Lustig W P, Zhang J, et al. *J. Am. Chem. Soc.*, **2015**, **137**:16209-16215
- [8] Lankshear M D, Beer P D. *Coord. Chem. Rev.*, **2006**,**250**:3142-3160
- [9] Ma L, Lin W. *J. Am. Chem. Soc.*, **2008**,**130**:13834-13835
- [10] Zheng B, Dong H, Bai J, et al. *J. Am. Chem. Soc.*, **2008**,**130**:7778-7779
- [11] Lin J B, Zhang J P, Zhang W X, et al. *Inorg. Chem.*, **2009**,**48**:6652-6660
- [12] Li S L, Tan K, Lan Y Q, et al. *Cryst. Growth Des.*, **2010**,**10**:1699-1705
- [13] Li C P, Du M. *Chem. Commun.*, **2011**,**47**:5958-5972
- [14] Su Z, Chen M, Okamura T A, et al. *Inorg. Chem.*, **2011**,**50**:985-991
- [15] Zhang Y, Yang J, Yang Y, et al. *Cryst. Growth Des.*, **2012**,**12**:4060-4071
- [16] Maity D K, Halder A, Bhattacharya B, et al. *Cryst. Growth Des.*, **2016**,**16**:1162-1167
- [17] Cui J W, An W J, Van Hecke K, et al. *Dalton Trans.*, **2016**, **45**:17474-17484
- [18] Mu Y, Han G, Li Z, et al. *Cryst. Growth Des.*, **2012**,**12**:1193-1200
- [19] Yang J, Ma J F, Liu Y Y, et al. *Inorg. Chem.*, **2007**,**46**:6542-6555
- [20] Ke C H, Lin G R, Kuo B C, et al. *Cryst. Growth Des.*, **2012**, **12**:3758-3765
- [21] Ke C H, Lee H M. *CrystEngComm*, **2012**,**14**:4157-4160
- [22] Vasylevskiy S I, Regeta K, Ruggi A, et al. *Dalton Trans.*, **2018**,**47**:596-607
- [23] Zhai L, Zhang W W, Ren X M, et al. *Dalton Trans.*, **2015**,**44**:5746-5754
- [24] Haldar R, Prasad K, Samanta P K, et al. *Cryst. Growth Des.*, **2016**,**16**:82-91
- [25] Gole B, Bar A K, Mallick A, et al. *Chem. Commun.*, **2013**,**49**:7439-7441
- [26] Wen H M, Li B, Yuan D Q, et al. *J. Mater. Chem. A*, **2014**,**2**:11516-11522
- [27] Liu J Y, Wang Q, Zhang L J, et al. *Inorg. Chem.*, **2014**,**53**:5972-5985
- [28] Wang C, Volotskova O, Lu K D, et al. *J. Am. Chem. Soc.*, **2014**,**136**:6171-6174
- [29] Fan C B, Zong Z, Meng X M, et al. *CrystEngComm*, **2019**,**21**:4880-4897
- [30] Arici M. *Cryst. Growth Des.*, **2017**,**17**:5499-5505
- [31] Lu B R, Li S B, Zhang X Z, et al. *New J. Chem.*, **2019**,**43**:15804-15810
- [32] Zeng C H. *Asian J. Chem.*, **2014**,**26**:7472-7474
- [33] Das K, Datta A, Mendiratta S, et al. *Inorg. Chem. Acta*, **2018**, **469**:478-483
- [34] Lee H J, Cheng P Y, Chen C Y. *CrystEngComm*, **2011**, **13**:4814-4816
- [35] Das K, Datta A, Mane S B, et al. *Chemistryselect*, **2016**, **1**:6230-6237
- [36] Li X, Yang L, Zhao L, et al. *Cryst. Growth Des.*, **2016**, **16**:4377-4382
- [37] Bruker. *SMART and SAINT, Program for Data Extraction and Reduction*, Bruker AXS, Inc., Madison, Wisconsin, USA, **2002**.
- [38] Sheldrick G M. *SADABS, Program for Empirical Absorption Correction of Area Detector Data*, University of Göttingen, Germany, **2003**.
- [39] Sheldrick G M. *SHELXS-2014, Program for Crystal Structure Solution*, University of Göttingen, Germany, **2014**.
- [40] Sheldrick G M. *SHELXL-2014, Program for the Refinement of Crystal Structure*, University of Göttingen, Germany, **2014**.
- [41] Addison A W, Rao T N, Reedijk J, et al. *J. Chem. Soc. Dalton Trans.*, **1984**:1349-1356
- [42] Nakamoto K. *Infrared and Raman Spectra of Inorganic and Coordinated Compounds. 5th Ed.* New York: Wiley & Sons, **1997**.
- [43] Cheng Y, Yang M L, Hu H M, et al. *J. Solid State Chem.*, **2016**,**239**:121-130
- [44] Bai C, Xu B, Hu H M, et al. *Polyhedron*, **2017**,**124**:1-11
- [45] Wu Y, Wu J, Luo Z D, et al. *RSC Adv.*, **2017**,**7**:10415-10423
- [46] Zhao X X, Wang S L, Zhang L Y, et al. *Inorg. Chem.*, **2019**, **58**:2444-2453
- [47] Roh S G, Kim Y H, Seo K D, et al. *Adv. Func. Mater.*, **2009**, **19**:1663-1671
- [48] Meng F D, Qin L, Zhang M D, et al. *CrystEngComm*, **2014**, **16**:698-706
- [49] Meng F D, Zhang M D, Shen K, et al. *Dalton Trans.*, **2015**, **44**:1412-1419
- [50] Wang F M, Zhou Z Y, Liu W, et al. *Dalton Trans.*, **2017**,**46**:956-961
- [51] Liu H Y, Wu H, Ma J F, et al. *Cryst. Growth Des.*, **2010**,**10**:4795-4805
- [52] Kan W Q, Liu Y Y, Yang J, et al. *CrystEngComm*, **2011**,**13**:4256-4269
- [53] Bai H Y, Yang J, Liu B, et al. *CrystEngComm*, **2011**,**13**:5877-5884
- [54] Yang J, Yuo Q, Li G D, et al. *Inorg. Chem.*, **2006**,**45**:2857-2865
- [55] Jin X H, Ren C X, Sun J K, et al. *Chem. Commun.*, **2012**,**48**:10422-10424
- [56] Xiao Y, Wang S H, Zhao Y P, et al. *CrystEngComm*, **2016**, **18**:2524-2531
- [57] Liu G N, Zhang M J, Liu W Q, et al. *Dalton Trans.*, **2015**,**44**:18882-18892
- [58] Liu G N, Zhu W J, Chu Y N, et al. *Inorg. Chim. Acta*, **2015**, **425**:28-35
- [59] Bauer C A, Timofeeva T V, Settersten T B, et al. *J. Am. Chem. Soc.*, **2007**,**129**:7136-7144
- [60] Doty F P, Bauer C A, Skulan A J, et al. *Adv. Mater.*, **2009**,**21**:95-101